Energy loss by charged particles in complex media

J. B. Pendry
The Blackett Laboratory, Imperial College, London SW7 2BZ, United Kingdom

L. Martín-Moreno
Instituto de Ciencia de Materiales (CSIC), Universidad Autónoma de Madrid, Cantoblanco, 28049, Madrid, Spain
(Received 24 January 1994)

The introduction of geometrical complexity into a dielectric structure radically alters the pattern of losses from a passing charged particle. Here we introduce an approach to the problem which is ideally suited to numerical work and to the treatment of complex geometry. We apply the method to losses in colloidal metallic systems where the local juxtaposition of surfaces produces a host of modes and consequent changes in the loss spectrum. We also calculate the "Smith-Purcell effect," in which a particle passing over a grating may radiate energy into the vacuum. This method is powerful and flexible and will, we trust, open a class of materials to quantitative study.

I. INTRODUCTION

Perhaps the most significant feature of interaction between fast charged particles and condensed matter is the energy loss they suffer. There are many regimes depending on the nature and speed of the particle, but we have in mind particles such as electrons traveling with velocities of the order $0.2c$. In this regime the losses are dominated by the dielectric properties of the medium and there is extensive literature on the subject: see Ref. 1 for further references. More recently there has been an interest in the more complex case of inhomogeneous media where structure is on the scale of nanometers. This geometric complexity radically changes the loss spectrum of the medium and there have been many attempts to relate the dielectric properties, the geometric structure, and the loss spectrum.[2–6] Mainly these attempts have been analytic studies based on some effective-medium theory of the generic Maxwell Garnett[7] type. These studies revealed that the shape of a material does indeed affect the electromagnetic modes involved in the loss process, particularly if the material is metallic.

Some success has attended these approaches, but it is generally accepted that there are difficulties in relating properties of the homogeneous effective medium to those of the actual inhomogeneous material on which the experiments are done. The problem is a difficult one because the electromagnetic fields inside an inhomogeneous medium often show violent spatial variations. For example, rough silver surfaces show giant Raman signals, indicating that local fields take values perhaps a thousand times the original incident field. Theorists have to be very careful about replacing such a highly inhomogeneous system with an equivalent homogeneous one and it is not surprising that difficulties have been encountered.

Despite the large amount of analytic work there seems to be a dearth of numerical studies, possibly due to absence of a suitable formulation of the problem. It is unfortunate that models are restricted to those which can be treated analytically. Numerical methods give the capacity to treat more complex systems and to provide a prescription for calculation of parameters used in effective-medium theories where these are appropriate. In this paper we give a formulation to the problem that is well suited to numerical work. Some examples are worked out in the later sections.

Our approach is one which builds up the effect of the medium in stages. We start with the charged particle in free space. If the particle is stationary, the fields around it are of a longitudinal nature, but as soon as it begins to move, the surrounding fields viewed in the laboratory frame become time dependent and can be described entirely in terms of the two time-dependent solutions of Maxwell's equations: the transverse modes. No energy is radiated by these transverse modes because the component of the wave vectors pointing away from the trajectory are always complex: the components of the wave field decay exponentially away from the particle's trajectory and so convey no energy to infinity.

So much for the vacuum, but the presence of a medium changes the nature of the surrounding field. We view this interaction as a scattering of the waves by the medium: essentially a diffraction and refraction phenomenon. Consider the simplest example of a particle traveling parallel to a surface. The evanescent waves emitted by the particle impinge upon the surface where they are reflected and refracted with or without diffraction according to the structure of the surface.

Refraction into the medium conserves momentum parallel to the surface, but changes the normal component. This leaves the possibility open that the component of momentum normal to the surface may no longer be complex: the evanescent waves may tunnel into the medium to find an energy carrying wave on the far side. For example, this can happen if the medium is glass and the particle is traveling faster than the velocity of light in glass. Then we couple by refraction to Cerenkov radiation in the glass, but with a probability that decays exponentially with the distance of the particle from the surface. At lower velocities the waves may still refract into an energy carrying mode. If the material is a metal, the surface plasmons will be excited and dissipate energy.

Diffraction introduces another ingenious way of coupling to energy carrying modes. It will be recalled that a particle *in vacuo* does not radiate because the balance between the frequency of the surrounding waves and their

components of momentum is wrong. Note that we are discussing diffraction of electromagnetic waves, not of the particle itself. From Maxwell's equations,

$$\omega^2=c^2(k_x^2+k_y^2+k_z^2)\ . \tag{1}$$

Let us choose the z axis normal to the surface so the momentum normal to the surface is given by

$$k_z=\pm i\sqrt{k_x^2+k_y^2-\omega^2c^{-2}} \tag{2}$$

and is normally complex *in vacuo* ensuring no radiation of energy. Diffraction at the surface can reduce k_x and k_y sufficiently for k_z to become real. Then the diffracted wave can carry energy to infinity, either radiating into the vacuum or into the material. A necessary condition is that the surface is not smooth, but has some lateral structure without which it cannot diffract waves. Smith and Purcell noted this effect some time ago.[8]

Yet another way in which energy loss can occur is through *multiple scattering* of the emitted waves. In a complex structure electromagnetic waves can rattle around between elements of the structure to form modes and resonances which the unstructured medium did not possess. A common example is colloidal silver in a photographic plate. Solid metallic silver does not have any substantial absorption bands in the visible and is highly reflecting to light. Colloidal silver traps light in very-low-frequency resonances between the colloidal particles,[9] which couple to and absorb incident light. These same resonances can couple to evanescent waves surrounding a moving charged particle and provide a multiple-scattering mechanism for the loss of energy.

This picture of light emitted by a moving charge to be scattered and diffracted by the medium is ideally suited to numerical calculation. A method of calculating the electromagnetic response of complex structures has been developed by Pendry and MacKinnon,[10,11] which can be harnessed to this approach to give realistic calculations of loss spectra for complex nanostructures.

In the next section we give mathematical expression to our formalism. In Sec. III we solve two old problems with the new method to show that it can perform the old tricks as well as some new ones. Finally we present calculations for complex metallic structures in which the stopping power is radically altered by the geometry of the material. We show how the loss spectrum of a metallic colloid changes dramatically with the dispersion and present strong evidence that, despite the complexity of the internal electromagnetic fields, an effective-medium theory does appear to be valid for these colloidal systems, though calculating the correct parameters is a tough job, one for which it is necessary to use our methods.

II. ENERGY LOSS BY CHARGED PARTICLES

A changed point particle is surrounded by an electromagnetic field which, through the Poynting vector, provides all information about electromagnetic losses of the particle. We begin with a stationary particle *in vacuo* and elaborate in stages until we have a prescription for the full electromagnetic field in a complex medium. The scalar and vector potentials in the rest frame of the particle are easily calculated:

$$\varphi(\mathbf{r})=\frac{q}{4\pi\varepsilon_0|\mathbf{r}|}\ ,\quad \mathbf{A}=\mathbf{0}\ . \tag{3}$$

Next we decompose into plane waves,

$$\varphi(\mathbf{r})=\frac{q}{4\pi\varepsilon_0|\mathbf{r}|}=\frac{q}{4\pi\varepsilon_0}\frac{(2\pi)^3}{2\pi^2L^3}\sum_{k_x,k_y,k_z}\frac{\exp(i\mathbf{k}\cdot\mathbf{r})}{k_x^2+k_y^2+k_z^2}\ ,$$

$$k_x=n_x\frac{2\pi}{L}\ , \tag{4}$$

etc. In the problems we treat here a particle travels parallel to the surface of a material, so we choose the z coordinate normal to that surface and the x coordinate along the direction of motion of the particle, assumed parallel to the surface. In fact it will be convenient to transform back into real space for the z coordinate,

$$\varphi(\mathbf{r})=\frac{q}{4\pi\varepsilon_0}\frac{(2\pi)^3}{4\pi^3L^2}\sum_{k_x,k_y}\int_{-\infty}^{+\infty}\frac{\exp(i\mathbf{k}\cdot\mathbf{r})}{(k_z+i\sqrt{k_x^2+k_y^2})(k_z-i\sqrt{k_x^2+k_y^2})}dk_z$$

$$=\frac{q}{4\pi\varepsilon_0}\frac{2\pi}{L^2}\sum_{k_x,k_y}\frac{\exp(i\mathbf{k}_\parallel\cdot\mathbf{r}_\parallel-\sqrt{k_x^2+k_y^2}|z|)}{\sqrt{k_x^2+k_y^2}}\ . \tag{5}$$

This choice of geometry is not as restrictive as it appears at first sight: we may treat a bulk problem by introducing *two* surfaces infinitesimally close together. A particle moving down a cylindrical hole could be treated either in a representation of cylindrical coordinates or in this surface representation with the surface chosen to cut the cylinder in half. A little ingenuity adapts our formulation to many geometries.

The Lorentz transformation

$$\mathbf{L}=\begin{bmatrix}\gamma & 0 & 0 & -i\beta\gamma\\ 0 & 1 & 0 & 0\\ 0 & 0 & 1 & 0\\ i\beta\gamma & 0 & 0 & \gamma\end{bmatrix}\ ,$$

$$\beta=v/c\ ,\quad \gamma=1/\sqrt{1-v^2/c^2} \tag{6}$$

gives us the fields in the laboratory frame in which the particle moves with velocity v, by acting on the following four-vectors giving the particle four-coordinates, the particle momentum/energy, and the electromagnetic fields. In the rest frame of the particle

$$X=\begin{bmatrix} x \\ y \\ z \\ ict \end{bmatrix}, \quad K=\begin{bmatrix} k_x \\ k_y \\ i\sqrt{k_x^2+k_y^2} \\ i\omega/c=0 \end{bmatrix}, \quad \Phi=\begin{bmatrix} cA_x=0 \\ cA_y=0 \\ cA_z=0 \\ i\varphi \end{bmatrix}. \tag{7}$$

In the laboratory frame

$$X'=\begin{bmatrix} \gamma x+v\gamma t \\ y \\ z \\ ic(\gamma t+vc^{-2}\gamma x) \end{bmatrix},$$

$$K'=\begin{bmatrix} \gamma k_x \\ k_y \\ i\sqrt{k_x^2+k_y^2} \\ i\omega'/c=+i\beta\gamma k_x \end{bmatrix}, \tag{8}$$

$$\Phi'=\begin{bmatrix} cA'_x=+\beta\gamma\varphi \\ 0 \\ 0 \\ i\gamma\varphi \end{bmatrix},$$

so that in the laboratory frame the fields look like

$$\Phi'=\begin{bmatrix} \beta\gamma \\ 0 \\ 0 \\ i\gamma \end{bmatrix} \frac{q}{4\pi\varepsilon_0}\frac{2\pi}{L^2}\sum_{k'_x,k'_y}\frac{\exp(ik'_x x'+ik'_y y'-\sqrt{\gamma^{-2}k'^2_x+k'^2_y}|z'|-i\omega' t')}{\sqrt{\gamma^{-2}k'^2_x+k'^2_y}}. \tag{9}$$

In other words, we have a set of electromagnetic waves radiating from the moving particle each with frequency proportional to the x component of momentum,

$$\omega'=\beta ck'_x=vk'_x. \tag{10}$$

We define dimensions for the Lorentz-contracted "box" containing the system

$$L'_x=L/\gamma, \quad L'_y=L \tag{11}$$

with momentum defined in the new frame by

$$k'_x=n_x\frac{2\pi}{L'_x}, \quad k'_y=n_y\frac{2\pi}{L'_y}. \tag{12}$$

Eventually in any calculation, we shall make an integration over k'_x,k'_y, or calculate a density of states and, the dimensions of the imaginary box will disappear. With these definitions the fields can be expressed entirely in terms of laboratory frame parameters

$$\Phi'=\begin{bmatrix} \beta \\ 0 \\ 0 \\ i \end{bmatrix} \frac{q}{4\pi\varepsilon_0}\frac{2\pi}{L'_xL'_y}\sum_{k'_x,L'_y}\frac{\exp(ik'_x x'+ik'_y y'-\sqrt{\gamma^{-2}k'^2_x+k'^2_y}|z'|-i\omega' t)}{\sqrt{\gamma^{-2}k'^2_x+k'^2_y}} \tag{13}$$

from which the scalar and vector potentials can be extracted,

$$\varphi'=\frac{q}{4\pi\varepsilon_0}\frac{2\pi}{L'_xL'_y}\sum_{k'_x,k'_y}\frac{\exp(ik'_x x'+ik'_y y'-\sqrt{\gamma^{-2}k'^2_x+k'^2_y}|z'|-i\omega' t)}{\sqrt{\gamma^{-2}k'^2_x+k'^2_y}}, \tag{14}$$

$$\mathbf{A}'=\begin{bmatrix} c^{-1}\beta=v/c^2 \\ 0 \\ 0 \end{bmatrix} \frac{q}{4\pi\varepsilon_0}\frac{2\pi}{L'_xL'_y}\sum_{k'_x,k'_y}\frac{\exp(ik'_x x'+ik'_y y'-\sqrt{\gamma^{-2}k'^2_x+k'^2_y}|z'|-i\omega' t')}{\sqrt{\gamma^{-2}k'^2_x+k'^2_y}}, \tag{15}$$

or, alternatively, the standard expressions

$$\mathbf{E}'=-\nabla'\varphi'-\partial\mathbf{A}'/\partial t', \quad \mathbf{B}'=\nabla'\times\mathbf{A}' \tag{16}$$

can be used to express the fields in the **E**−**B** format

$$\mathbf{E}'=\frac{q}{2\varepsilon_0 L_x' L_y'}\sum_{k_x',k_y'}\begin{bmatrix}-ik_x'+i\omega' vc^{-2}\\ -ik_y'\\ (z'/|z'|)\sqrt{\gamma^{-2}k_x'^2+k_y'^2}\end{bmatrix}\frac{\exp(ik_x'x'+ik_y'y'-\sqrt{\gamma^{-2}k_x'^2+k_y'^2}|z'|-i\omega' t')}{\sqrt{\gamma^{-2}k_x'^2+k_y'^2}}, \tag{17}$$

$$\mathbf{B}'=\frac{vq}{2c^2\varepsilon_0 L_x' L_y'}\sum_{k_x',k_y'}\begin{bmatrix}0\\ -(z'/|z'|)\sqrt{\gamma^{-2}k_x'^2+k_y'^2}\\ -ik_y'\end{bmatrix}\frac{\exp(ik_x'x'+ik_y'y'-\sqrt{\gamma^{-2}k_x'^2+k_y'^2}|z'|-i\omega' t')}{\sqrt{\gamma^{-2}k_x'^2+k_y'^2}}. \tag{18}$$

The requirement that a particle in uniform motion *in vacuo* does not radiate is met by the condition that k_z' is always complex, implying that waves decay away exponentially from the plane containing the particle. By implication they carry no energy flux. The presence of a medium close to the plane can change this situation either by allowing evanescent waves to tunnel through the vacuum into allowed states of the medium, such as surface plasmon modes, or by diffracting an evanescent wave into a propagating wave with real k_z, which may then carry flux away from the plane of the particle. This last effect was noted some time ago by Smith and Purcell.

In a recent work[10,11] Pendry and MacKinnon described a powerful formalism that enabled the reflection coefficient of a surface to be calculated. Consider a charged particle traveling parallel to the surface of the material. Figure 1 shows the situation.

Using the Pendry-MacKinnon formalism we can calculate the reflection coefficient of the surface, but first we need to introduce some notation. Conventionally electromagnetic waves at surfaces are described in terms of amplitudes of *S*- and *P*-polarized waves. The *S*-polarized wave has an **E** vector lying entirely in the plane of the surface,

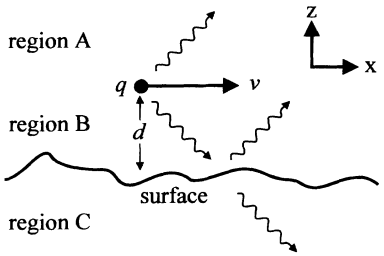

FIG. 1. A particle, charge q, moves with velocity v parallel to the surface of a dielectric medium at a distance d. The charge initially radiates evanescent electromagnetic waves, but these may be refracted at the surface into propagating modes within the medium which carry energy away from the particle. Alternatively the waves may be diffracted at the surface into a wave which propagates *in vacuo* and carries energy away from the particle, but this time into free space.

$$\mathbf{E}_S'^{\pm}(k_x',k_y',z',\omega')=\begin{bmatrix}k_y'\\ -k_x'\\ 0\end{bmatrix}\exp(ik_x'x'+ik_y'y'\pm ik_z'z'-i\omega' t'),$$

$$\mathbf{B}_S'^{\pm}(k_x',k_y',z',\omega')=\frac{1}{\omega'}\begin{bmatrix}\pm k_x'k_z'\\ \pm k_y'k_z'\\ -k_x'^2-k_y'^2\end{bmatrix}\exp(ik_x'x'+ik_y'y'\pm ik_z'z'-i\omega' t'), \tag{19}$$

where ± denotes waves heading away from or towards the surface and k_z is determined by the usual vacuum dispersion relation

$$\begin{aligned}k_z'&=+\sqrt{\omega'^2c^{-2}-k_x'^2-k_y'^2}, \quad \omega'^2c^{-2}>k_x'^2+k_y'^2\\ k_z'&=+i\sqrt{k_x'^2+k_y'^2-\omega'^2c^{-2}}, \quad \omega'^2c^{-2}<k_x'^2+k_y'^2.\end{aligned} \tag{20}$$

The *P*-polarized wave has the **E** vector lying in the plane containing **k** and the surface normal,

$$\mathbf{E}_P'^{\pm}(k_x',k_y',z',\omega')=\frac{-c^2}{\omega'}\begin{bmatrix}\pm k_x'k_z'\\ \pm k_y'k_z'\\ -k_x'^2-k_y'^2\end{bmatrix}\times\exp(ik_x'x'+ik_y'y'\pm ik_z'z'-i\omega' t'), \tag{21}$$

$$\mathbf{B}_P'^{\pm}(k_x',k_y',z',\omega')=\begin{bmatrix}k_y'\\ -k_x'\\ 0\end{bmatrix}\exp(ik_x'x'+ik_y'y'\pm ik_z'z'-i\omega' t').$$

We project the waves emitted towards the surface by the particle onto the *SP* basis as follows:

$$\mathbf{F}'=\sum_{k_x',k_y'}\{A_S^-(k_x',k_y')\mathbf{F}_S^-(k_x',k_y',z',\omega'=vk_x') + A_P^-(k_x',k_y')\mathbf{F}_P^-(k_x',k_y',z',\omega'=vk_x')\}\ , \tag{22}$$

where $\mathbf{F}$ is a six-vector comprising both $\mathbf{E}$ and $\mathbf{B}$ and the amplitudes are given by

$$A_S^{\pm}=\frac{iqv^2c^{-2}k_x'k_y'}{2\varepsilon_0 L_x'L_y'(k_x'^2+k_y'^2)\sqrt{\gamma^{-2}k_x'^2+k_y'^2}}\ ,$$
$$A_P^{\pm}=\frac{\pm vqk_x'}{2c^2\varepsilon_0 L_x'L_y'(k_x'^2+k_y'^2)}\ . \tag{23}$$

Using our formalism to calculate surface reflectivity we can find the total wave field in region B, between surface and particle,

$$\mathbf{F}'_B=\sum_{k_x',k_y'}A_S^-(k_x',k_y')\mathbf{F}_S^-(k_x',k_y',z',\omega'=vk_x')+A_P^-(k_x',k_y')\mathbf{F}_P^-(k_x',k_y',z',\omega'=vk_x') + \sum_{k_x'',k_y''}B_S(k_x'',k_y'')\mathbf{F}_S^+(k_x'',k_y'',z',\omega'=vk_x')+B_P(k_x'',k_y'')\mathbf{F}_P^+(k_x'',k_y'',z',\omega'=vk_x')\ , \tag{24}$$

where the reflected amplitudes are given by

$$B_S(k_x'',k_y'')=\exp(-d\sqrt{\gamma^{-2}k_x'^2+k_y'^2}-d\sqrt{k_x''^2-\beta^2k_x'^2+k_y''^2}) \times\{R_{SS}(k_x'',k_y'';k_x',k_y';\omega'=vk_x')A_S^-(k_x',k_y')+R_{SP}(k_x'',k_y'';k_x',k_y';\omega'=vk_x')A_P^-(k_x',k_y')\}$$
$$B_P(k_x'',k_y'')=\exp(-d\sqrt{\gamma^{-2}k_x'^2+k_y'^2}-d\sqrt{k_x''^2-\beta^2k_x'^2+k_x''^2}) \times\{R_{PS}(k_x'',k_y'';k_x',k_y';\omega'=vk_x')A_S^-(k_x',k_y')+R_{PP}(k_x'',k_y'';k_x',k_y';\omega'=vk_x')A_P^-(k_x',k_y')\}\ . \tag{25}$$

The distance of the particle trajectory from the surface is d. Note the subtlety of these expressions: the surface may change momenta of incident waves, but not their frequency. On the other hand, the frequency is linked to k_x' for the *incident* wave.

Similarly we may find the total wave field in region A, on the far side of the particle from the surface,

$$\mathbf{F}'_A=\sum_{k_x',k_y'}\left\{A_S^+(k_x',k_y')\mathbf{F}_S^+(k_x',k_y',z',\omega'=vk_x')+A_P^+(k_x',k_y')\mathbf{F}_P^+(k_x',k_y',z',\omega'=vk_x') + \sum_{k_x'',k_y''}B_S(k_x'',k_y'')\mathbf{F}_S^+(k_x'',k_y'',z',\omega'=vk_x')+B_P(k_x'',k_y'')\mathbf{F}_P^+(k_x'',k_y'',z',\omega'=vk_x')\right\}\ . \tag{26}$$

We have assumed that the particle does not scatter the reflected waves a second time, which is equivalent to assuming that the particle is either very massive or travels very quickly so that its trajectory is not perturbed by the presence of the surface.

This completes our formal derivation of the electromagnetic fields. We can use our expressions to calculate the Poynting vector in region A, which gives energy flux out in the vacuum, or in region B, which gives energy flux into the surface.

III. TWO SIMPLE EXAMPLES

In an earlier paper Echenique and Pendry[2] showed how to calculate the rate of energy loss by a particle traveling parallel to a smooth flat metal surface. They showed that the rate of loss of energy to the surface plasmons is given by

$$\int \mathbf{N}_z\,dx\,dy = \int\int \frac{vq^2k_x'}{8\pi^2\varepsilon_0\sqrt{k_x'^2+k_y'^2}}\exp(-2d\sqrt{k_x'^2+k_y'^2}) \times\mathrm{Im}\left[\frac{1-\varepsilon_2(\omega'=vk_x')}{1+\varepsilon_2(\omega'=vk_x')}\right]dk_x'dk_y'\ . \tag{27}$$

We rederive this result using our formalism as follows. The reflection coefficients of a dielectric surface are given by

$$R_{SS}=\frac{\sqrt{\varepsilon_1}\cos(\theta_i)-\sqrt{\varepsilon_2}\cos(\theta_r)}{\sqrt{\varepsilon_1}\cos(\theta_i)+\sqrt{\varepsilon_2}\cos(\theta_r)}\ ,$$
$$R_{PP}=-\frac{\sqrt{\varepsilon_1}\cos(\theta_r)-\sqrt{\varepsilon_2}\cos(\theta_i)}{\sqrt{\varepsilon_1}\cos(\theta_r)+\sqrt{\varepsilon_2}\cos(\theta_i)}\ , \tag{28}$$

where, in our case,

$$\varepsilon_1=1\ , \tag{29}$$

and the angles are given in terms of the momentum

$$\cos(\theta_i)=\frac{i\sqrt{(1-v^2c^{-2})k_x^2+k_y^2}}{vc^{-1}k_x}\ ,$$
$$\cos(\theta_r)=\frac{i\sqrt{(1-v^2\varepsilon_2c^{-2})k_x^2+k_y^2}}{vc^{-1}\sqrt{\varepsilon_2}k_x}\ . \tag{30}$$

We shall model the dielectric constant of the metal with a single plasmon pole

$$\varepsilon_2=1-\omega_p^2/\omega^2\ . \tag{31}$$

The reflection coefficients are then

$$R_{SS}=\frac{\sqrt{(1-v^2c^{-2})k_x^2+k_y^2}-\sqrt{(1-v^2\varepsilon_2c^{-2})k_x^2+k_y^2}}{\sqrt{(1-v^2c^{-2})k_x^2+k_y^2}+\sqrt{(1-v^2\varepsilon_2c^{-2})k_x^2+k_y^2}}\ ,$$
$$R_{PP}=-\frac{\sqrt{(1-v^2\varepsilon_2c^{-2})k_x^2+k_y^2}-\varepsilon_2\sqrt{(1-v^2c^{-2})k_x^2+k_y^2}}{\sqrt{(1-v^2\varepsilon_2c^{-2})k_x^2+k_y^2}+\varepsilon_2\sqrt{(1-v^2c^{-2})k_x^2+k_y^2}}\ . \tag{32}$$

At this point our calculations are fully relativistic and include retardation, which can be important in some circumstances; see Refs. 12–14. The original calculations were made in the electrostatic limit, which corresponds to neglecting terms of order v^2c^{-2}. In this limit,

$$R_{SS}\approx 1\ ,\quad R_{PP}\approx -\frac{1-\varepsilon_2}{1+\varepsilon_2}=\frac{-\omega_p^2}{2\omega^2-\omega_p^2}\ . \tag{33}$$

We observe that both the incident waves and the reflected waves are evanescent and in consequence no energy can flow towards the surface unless the reflection coefficient has an imaginary component. Thus the S wave makes no contribution, but the P wave does at the surface plasmon pole,

$$1+\varepsilon_2=0\ \text{ or }\ \omega=\pm\omega_p/\sqrt{2}\ . \tag{34}$$

Thus the P component of the wave in region B is

$$\mathbf{F}'_{BP}\approx\sum_{k'_x,k'_y}A_P^-(k'_x,k'_y)\times\{\mathbf{F}_P^-(k'_x,k'_y,\omega'=vk'_x)+R_{PP}(\omega'=vk'_x)\exp(-2d\sqrt{k_x'^2+k_y'^2})\times\mathbf{F}_P^+(k'_x,k'_y,\omega'=vk'_x)\}\ . \tag{35}$$

Evaluating the Poynting vector for this field gives a flow of energy into the surface (see Appendix A):

$$\int\mathbf{N}_z\,dx\,dy=\int(\mathbf{E}\times\mathbf{H})_z\,dx\,dy=\int(E_xH_y-E_yH_x)\,dx\,dy=\int\int\frac{vq^2k'_x}{8\pi^2\varepsilon_0\sqrt{k_x'^2+k_y'^2}}\exp(-2d\sqrt{k_x'^2+k_y'^2})\,\mathrm{Im}\left[\frac{1-\varepsilon_2(\omega'=vk'_x)}{1+\varepsilon_2(\omega'=vk'_x)}\right]dk'_x\,dk'_y\ , \tag{36}$$

in agreement with Echenique and Pendry. Retaining the relativistic terms leads to a slightly more complex calculation, the result of which is

$$\int\mathbf{N}_z^{\mathrm{rel}}\,dx\,dy=\int(\mathbf{E}\times\mathbf{H})_z\,dx\,dy=\int(E_xH_y-E_yH_x)\,dx\,dy=\int\int\frac{vq^2k'_x}{8\pi^2\varepsilon_0}\frac{\exp(-2dp)}{p}\,\mathrm{Im}\left[\frac{2-\varepsilon_2-\alpha}{\varepsilon_2+\alpha}-\beta^2\frac{1-\alpha}{1+\alpha}\right]dk'_x\,dk'_y\ , \tag{37}$$

where

$$p\equiv\sqrt{k_x'^2\gamma^{-2}+k_y'^2}\ ,$$
$$\alpha\equiv\frac{\sqrt{k_x'^2+k_y'^2-\varepsilon_2\beta^2k_x'^2}}{\sqrt{k_x'^2+k_y'^2-\beta^2k_x'^2}}\ , \tag{38}$$
$$\varepsilon_2\equiv\varepsilon_2(\omega'=vk'_x)\ .$$

Our method of calculating the energy loss appears to be based entirely in the vacuum and therefore is concerned with the transverse modes of the vacuum. At first sight this appears to preclude treating losses to longitudinal modes of the bulk. But this is not the case. Energy loss by charged particles traversing the bulk of a material can be calculated by considering the limit of two surfaces pressed infinitesimally close together; see Fig. 2. In this

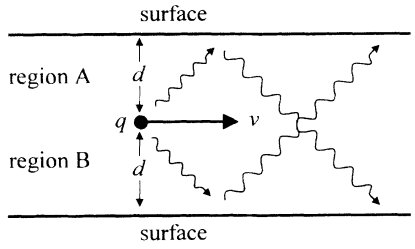

FIG. 2. A particle, charge q, moves with velocity v between two parallel surfaces of a dielectric medium at a distance d from each. The evanescent electromagnetic waves radiated by the charge multiply scatter between the two surfaces altering the resonant surface plasma frequency. In the limit $d \to 0$ absorption of energy occurs entirely at the *bulk* plasma frequency, as we expect when no surface is actually present.

case the waves emitted by the charged particle scatter alternately from one surface then the other so that the total wave field is more complicated,

$$\mathbf{F}'_{BP} \approx \sum_{k'_x,k'_y} A_P^-(k'_x,k'_y)\mathbf{F}_P^-(k'_x,k'_y,\omega'=vk'_x) \times \frac{1}{1+R_{PP}\exp(-2d\sqrt{k_x'^2+k_y'^2})} + A_P^-(k'_x,k'_y)\mathbf{F}_P^+(k'_x,k'_y,\omega'=vk'_x) \times \frac{R_{PP}\exp(-2d\sqrt{k_x'^2+k_y'^2})}{1+R_{PP}\exp(-2d\sqrt{k_x'^2+k_y'^2})} . \quad (39)$$

Losses occur when the integrand has a pole due to zero in the denominator of the fraction. The frequency of these losses now varies strongly with parallel momentum. In the limit $d \to 0$ the losses converge on the bulk plasma frequency

$$0 = 1+R_{PP} = \frac{2\varepsilon_2}{1+\varepsilon_2} = \frac{2(1-\omega_p^2/\omega^2)}{(2-\omega_p^2/\omega^2)} \quad (40)$$

and the rate of energy loss calculated from the Poynting vector in region B, Fig. 2, is (see Appendix B)

$$\int \mathbf{N}_z dx\,dy = \int (E_x H_y - E_y H_x)dx\,dy = \int\int \frac{vq^2k'_x}{2c^2\varepsilon_0^2\mu_0\sqrt{k_x'^2+k_y'^2}} \mathrm{Im}\frac{1-R_{PP}(\omega'=vk'_x)\exp(-2d\sqrt{k_x'^2+k_y'^2})}{1+R_{PP}(\omega'=vk'_x)\exp(-2d\sqrt{k_x'^2+k_y'^2})} dk'_x dk'_y \quad (41)$$

or, in the limit of zero separation between the surfaces,

$$2\int \mathbf{N}_z dx\,dy = 2\int (E_x H_y - E_y H_x)dx\,dy = \int\int \frac{vq^2k'_x}{4\pi^2\varepsilon_0\sqrt{k_x'^2+k_y'^2}} \times \mathrm{Im}\frac{1}{\varepsilon_2(\omega'=vk'_x)} dk'_x dk'_y , \quad (42)$$

in agreement with the result given by Landau and Lifshitz.[15]

Thus we have established that we have a complete formalism that reproduces results of earlier analytic work and which is ideally suited for application to more complex systems where analytic approaches break down.

IV. LOSSES IN COLLOIDAL METALS

It has been recognized that nanoscale structure in a medium profoundly affects its loss spectroscopy, particularly when the material is a metal. The reasons are well understood in principle: long-range electrostatic interaction of the plasma modes leads to a complex spectrum of new modes. However, the details have been more difficult to establish. Experiments on colloidal dispersions[16] show, in addition to the bulk plasma loss, strongly broadened features centered around the plasma dipole mode of a sphere and there have been many analytic attempts to model the observed spectra. The modes of a sphere have been invoked[3-5] as have the modes of coupled spheres[17] and more complex geometries.[18] Another approach has been to try to establish an effective-medium theory along the lines of Maxwell Garnett.[7] These approaches have met with some success, but there is a general failure to describe the complexity of the spectra with any precision.

In this paper we offer our computational approach as a tool for the study of these systems. Our objective is to show that the method can indeed calculate loss spectra for complex systems and to make some general observations about the nature of these spectra. We make some limited comparisons to the data of Howie and Walsh,[16] though it is not our purpose in this paper to give a comprehensive account of experimental loss spectra, but rather to establish how we might go forward to do this in the future.

We calculate for two systems. The first system comprises electrons traveling at 0.4c, 1 nm above, and perpendicular to, a set of aluminum cylinders where the cylinders have a diameter of 2.5 nm and are arranged in a square array lattice constant 5.0 nm giving a volume filling fraction of 19.6%. Figure 3 shows a sketch of the

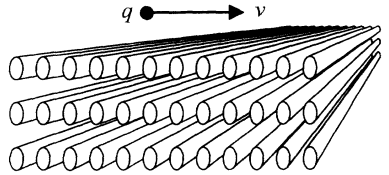

FIG. 3. A particle, charge q, moves with velocity v parallel to a surface comprising a regular array of metal cylinders, with a diameter of 2.5 nm, at a distance of 1 nm from the surface. The lattice spacing of the cylinders is 5.0 nm and the particle travels perpendicular to the cylinders at 0.4c. The volume filling fraction is 19.6%

system. Zabala and Echenique have also made calculations for cylindrical geometries.[19] The dielectric properties of aluminum are modeled as follows:

$$\varepsilon = 1 - \frac{\omega_p^2}{\omega(\omega + i\gamma)} , \quad \hbar\omega_p = 15 \text{ eV} , \quad \hbar\gamma = 1 \text{ eV} . \tag{43}$$

We calculate the reflection coefficient of this surface to the relevant waves, this time numerically because the system is not tractable to analytic study, and calculate the stopping power as a function of the energy of the modes causing the loss of energy. The results are shown in Fig. 4.

Note the dramatic effect that the nanoscale cylindrical structure has had on the loss spectrum. Equation (37) predicts that a smooth flat surface of aluminum would show losses close to the surface plasmon frequency of 10.6 eV, but here we see a whole spectrum of losses extending from zero up to the bulk plasmon frequency. The character of the spectrum is established in broad outline with only one layer of cylinders indicating that the modes excited are rather strongly localized between two cylinders. The insensitivity to the number of layers indicates that the loss spectrum is dictated by spacing between pairs of cylinders rather than the exact nature of the period lattice we have chosen.

In a second calculation the array of cylinders was replaced by an array of spheres with a diameter of 2.5 nm arranged in a simple cubic lattice of side of 5 nm giving a volume filling fraction of 6.5%. An electron travels at $0.4c$ parallel to the (100)axis, 1 nm above a (001) surface of this material. The situation is shown in Fig. 5. The corresponding loss spectrum is shown in Fig. 6. Once again we observe a wide spectrum that is established with the first layer of the material. The loss modes of a sphere are given by

$$\omega_{\text{sphere}} = \omega_p \left[\frac{l}{2l+1} \right]^{1/2} , \tag{44}$$

where l is a positive integer, with the dipole mode being found at 8.7 eV in the case of aluminum. The simple cubic lattice shows a broad double-peak structure with the stronger of the two peaks at 6.2 eV.

Our calculations indicate, both in the cylinder and the sphere cases, that the loss spectrum depends only on the most simplistic parameters of the lattice such as the proximity of the spheres or cylinders. This leads to two speculations. The first is that a wide range of nanostructures may well give rise to similar spectra provided that the *local* geometry of the objects is the same. Thus a colloidal dispersion of metallic spheres might be modeled by an ordered lattice of spheres of the same diameter at the same volume filling fraction. The other speculation is that the nanostructure can be replaced by an homogeneous effective medium. This is the objective of the Maxwell Garnett class of theories.

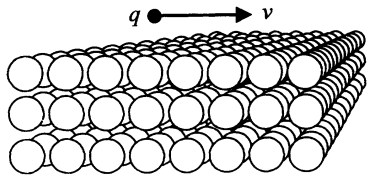

FIG. 5. A particle, charge q, moves with velocity v parallel to a surface comprising a simple cubic array of metal spheres, with a diameter of 2.5 nm, at a distance of 1 nm from the surface. The lattice spacing of the spheres is 5.0 nm and the particle travels parallel to the (100) axis of the lattice at $0.4c$. The volume filling fraction is 6.5%.

Let us deal with the latter speculation first. We have a very effective way of testing the postulate: if the nanostructured medium can truly be replaced by an effective homogeneous medium, then the response of that medium is determined by the two electromagnetic modes supported by such a homogeneous system. To test this hypothesis we calculated the band structure of the simple cubic lattice of metal spheres and asked if the losses were dominated by a single pair of Bloch waves. It is indeed the case that over the entire range of energies a single pair is dominant and we used the dispersion relation of these Bloch waves along the (001) direction to define an effective dielectric constant

$$\omega\varepsilon_{\text{eff}}(\omega) = ck_z(\omega) . \tag{45}$$

In Fig. 7 we show the full loss spectrum calculation for six layers of spheres compared to $\text{Im}(1/\varepsilon_{\text{eff}})$.

The agreement between the two curves is excellent, especially so as we took very little care about which Bloch waves we chose for our estimate of ε_{eff}. Clearly the effective-medium concept works extremely well in this in-

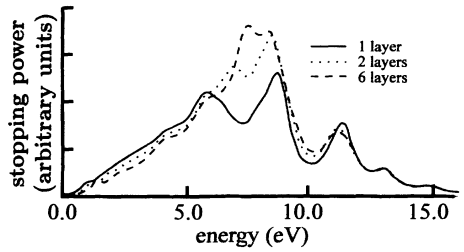

FIG. 4. The stopping power of the surface described in Fig. 3 as a function of the energy of the quanta lost. Note the very broad loss peak, which indicates a wide spectrum of modes extending to zero energy. The character of the loss spectrum is established almost with the first layer of cylinders in place indicating that the loss modes are very localized.

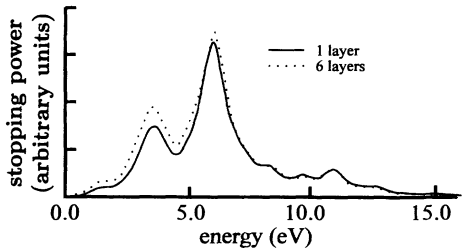

FIG. 6. The stopping power of the surface described in Fig. 5 as a function of the energy of the quanta lost. Again note the very broad loss peak, which indicates a wide spectrum of modes extending to zero energy. As for the cylinders, the character of the loss spectrum is established almost with the first layer, indicating that the loss modes are very localized.

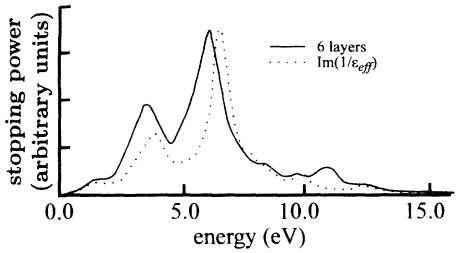

FIG. 7. The stopping power of the surface described in Fig. 5 as a function of the energy of the quanta lost calculated for six layers of spheres compared to $\mathrm{Im}(1/\varepsilon_{\mathrm{eff}})$ as defined by the Bloch waves of the system. The detailed agreement shows that effective-medium theory works very well for this system.

stance. We also have found a relatively simple procedure for calculating $\varepsilon_{\mathrm{eff}}$, something which has proved an elusive quantity within the entirely analytic approaches. Figure 8 shows some more calculations of $\mathrm{Im}(1/\varepsilon_{\mathrm{eff}})$ made for various filling fractions. We see that the trend with increasing filling fraction is for the loss peak to move to higher energies with the bulk plasma frequency as a limit point. This is consistent with the expectations that in the limit of 100% filling fraction all losses would be due to the bulk plasmon.

Now let us return to the first speculation: that only the local geometry of the nanostructure affects the loss spectrum. We have strong circumstantial evidence for this from our calculations. As we have seen, details of the spectrum are established by as little as one layer thickness of the material. Furthermore, although the losses excite many Bloch plasma waves traveling in all directions inside the material, a crude sampling of only one direction gives most of the details in the loss spectrum. As a further test of our ideas we refer to some data taken by Howie and Walsh.[16] They measured losses in an electron microscope with an AlF_3 sample on the stage. Decomposition in the electron beam gave an aluminum colloid. Comparison of their data with Fig. 8 shows that a filling fraction of approximately 12% best fits their data. A detailed comparison is shown in Fig. 9.

The experimental data show a broad peak centered on 8 eV, which is due to the surface modes of the spheres, and a well-defined peak at around 15 eV, which has a trivial origin in the bulk plasmon loss. Here we are not concerned with the latter, which we could easily repro-

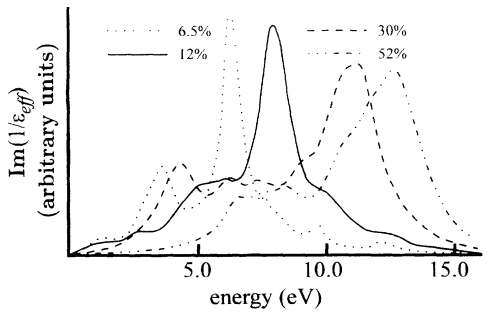

FIG. 8. The stopping power of the surface described in Fig. 5 as a function of the energy of the quanta lost estimated by $\mathrm{Im}(1/\varepsilon_{\mathrm{eff}})$ as defined by the Bloch waves of the system. Various filling fractions are shown obtained by varying the radius of the metallic spheres.

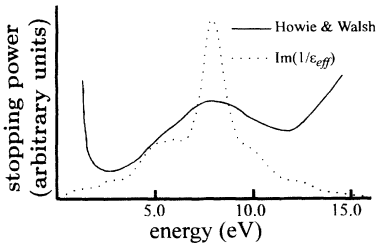

FIG. 9. The stopping power of a 12% colloidal dispersion of metallic spheres estimated by $\mathrm{Im}(1/\varepsilon_{\mathrm{eff}})$ and compared to electron energy loss data taken by Howie and Walsh. The scales are in arbitrary units for both theory and experiment. The experimental data show a broad peak at 8 eV, in agreement with the calculation. The peak at the origin in the experimental data is due to the finite resolution of the apparatus. There is also a bulk plasmon loss evident in the experimental data at around 15 eV which is due to the electron trajectories intersecting some of the colloidal spheres.

duce by averaging over trajectories intersecting the colloidal spheres. Our theory shows good agreement with the 8-eV peak both in location (which admittedly we have chosen the dispersion to fit) and more significantly in the width which shows the dispersion of modes over many frequencies. This result is very encouraging confirmation that real nanostructured materials can be modeled by our calculations.

A word of caution is in order: since the loss modes in a colloid are determined by local arrangement of spheres, we may expect to describe these losses if our model contains spheres with separations similar to those in the experiments. The system appears to be very tolerant of the range of separations: a given dispersion of the particle produces a broadband of modes which is well described by some average spacing. The exception to this statement comes at the limits of the spectrum. Here the random system will have many more modes than the ordered one because the random system has occasional sphere-sphere separations which are very small and which will produce low-frequency modes not present in the ordered system. For systems we describe here we expect that our ordered model will reproduce losses in the infrared region and beyond. The model appears to provide a good description of losses in the visible region which is in the central region of the spectrum where statistics are good.

V. THE SMITH-PURCELL EFFECT

So far we have concentrated our efforts on energy loss from the particle to the medium, but it is also possible for energy to escape into the vacuum. As we have pointed out, the charged particle radiates electromagnetic waves of all frequencies, but with a complex z component of the wave vector, which precludes radiation of energy. The reason that the wave vector is complex is that the frequency is related to the x component of the momentum

$$\omega = v k_x \tag{46}$$

in just such a way as to ensure that

$$k_z = \sqrt{\omega^2 c^{-2} - k_x^2 - k_y^2} \tag{47}$$

is always complex. If some means could be found to reduce k_x by a sufficient amount, k_z would once more be

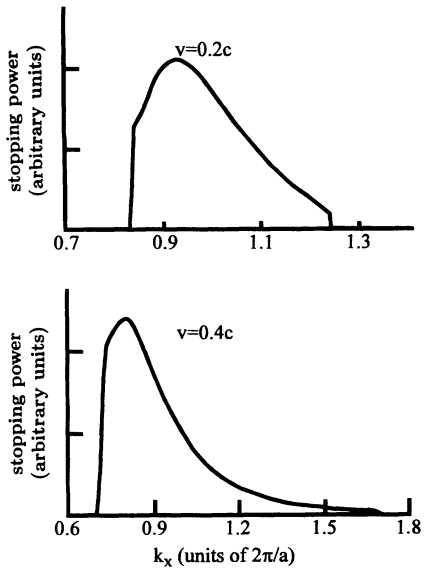

FIG. 10. The first-harmonic Smith-Purcell contribution to the stopping power of a 1D array of aluminum cylinders, with a diameter of 2.5 nm and spacing of 5.0 nm. An electron passes over the grating at right angles to the cylinders, at a height of 1 nm and a speed of $0.2c$ or $0.4c$. Emission takes place over a finite range of frequencies (as determined by k_x) in the self-x-ray region from 259 to 390 eV in the former case and from 436 to 1060 eV in the latter case.

real enabling the radiated wave to carry energy. One way of doing this is to diffract the emitted wave from a periodic grating which supplies discrete units of momentum. If

$$k_z=\sqrt{\omega^2c^{-2}-(k_x-g)^2-k_y^2} \tag{48}$$

is real, the condition for radiation is met.

This is our way of looking at the problem, but it has been pointed out to us[20] that Smith and Purcell have an alternative interpretation.[8] They considered the image of the charge in the dielectric. If the surface of the dielectric is not flat, the image will move up and down as the particle passes over the surface: this classic oscillating dipole will radiate energy into the vacuum. The two pictures are complementary: Smith and Purcell give an intuitive picture of where the energy comes from; our picture leads directly to an elegant and straightforward calculation of how much energy is radiated.

To illustrate the situation we considered a grating consisting of a one-dimensional array of aluminum cylinders, with a diameter of 2.5 nm and spacing of 5.0 nm, as before. An electron passes over the grating at right angles to the cylinders, at a height of 1 nm and a speed of $0.4c$. There is a range of momenta over which radiation can be expected given by the following condition:

$$(k_x-2\pi n/a)^2<k_x^2v^2c^{-2}$$
or
$$(\omega/v-2\pi n/a)^2<\omega^2c^{-2}\ , \tag{49}$$

where we have recognized that g is related to the lattice spacing through an integer n and that the frequency is proportional to k_x. In Fig. 10 we see the contribution to the stopping power from the Smith-Purcell effect, integrated over k_y.

VI. CONCLUSIONS

We have introduced a way of looking at energy loss from fast charged particles that opens the way to numerical studies with complex structure on a nanometer scale. Such structure radically alters the loss spectrum of the material. We have applied the formalism to some simple analytic calculations to show that it reproduces well-known results and to some numerical studies of losses in periodic arrays of nanometer sized metallic spheres. These systems displayed properties that were strongly dependent on the concentration of metal in the system and we used the periodic system successfully to model losses measured in colloidal aluminum where the arrangement of spheres is random, characterized only by the concentration of metal. We justified this approach by the insensitivity of the calculations to details of the order and to the validity of effective-medium theory, which we were able to demonstrate for this system, albeit with parameters which are difficult to determine. Finally we demonstrated the Smith-Purcell effect in which a charged particle moving over a grating radiates energy into the vacuum.

We hope that our method will prove applicable to quantitative studies of loss processes in complex materials, many of which are currently under experimental study.

ACKNOWLEDGMENTS

J.B.P. thanks Pedro Echenique and Archie Howie, who first drew his attention to the difficult problem of losses in nanostructures. L.M.M. thanks Imperial College, where this work was carried out, for its hospitality, and the Comisión Interministerial de Ciencia y Tecnología of Spain for financial support. We both thank Bob Greenler, who made us aware of the work of Smith and Purcell.

APPENDIX A

Here are the components of the fields for a charged particle traveling parallel to a flat metal surface:

$$E_x(z=-0)=\sum_{k_x',k_y'} A_P^-(k_x',k_y')\frac{c^2}{\omega'}k_x'k_z'\exp(ik_x'x+ik_y'y-i\omega' t)[1-R_{PP}(\omega'=vk_x')\exp(-2d\sqrt{k_x'^2+k_y'^2})]\ ,$$

$$E_y(z=-0)=\sum_{k_x',k_y'} A_P^-(k_x',k_y')\frac{c^2}{\omega'}k_y'k_z'\exp(ik_x'x+ik_y'y-i\omega' t)[1-R_{PP}(\omega'=vk_x')\exp(-2d\sqrt{k_x'^2+k_y'^2})]\ , \tag{A1}$$

$$B_x(z=-0)=\sum_{k_x',k_y'} A_P^-(k_x',k_y')(k_y')\exp(ik_x'x+ik_y'y-i\omega' t)[1+R_{PP}(\omega'=vk_x')\exp(-2d\sqrt{k_x'^2+k_y'^2})] ,$$

$$B_y(z=-0)=\sum_{k_x',k_y'} A_P^-(k_x',k_y')(-k_x')\exp(ik_x'x+ik_y'y-i\omega' t)[1+R_{PP}(\omega'=vk_x')\exp(-2d\sqrt{k_x'^2+k_y'^2})] .$$

Next we recognize that integration over xy leads to $k_B=-k_E$ and that the overall fields must be real

$$\begin{aligned}\int \mathbf{N}_z dx\,dy &= \int (E_xH_y-E_yH_x)dx\,dy \\ &= \sum_{k_x',k_y'} \left|A_P^-(k_x',k_y')\right|^2 \frac{c^2L_x'L_y'}{vk_x'} k_x' i\sqrt{k_x'^2+k_y'^2}\mu_0^{-1}(+k_x') \\ &\quad\times[1-R_{PP}(\omega'=+vk_x')\exp(-2d\sqrt{k_x'^2+k_y'^2})][1+R_{PP}(\omega'=-vk_x')\exp(-2d\sqrt{k_x'^2+k_y'^2})] \\ &\quad-\sum_{k_x',k_y'} \left|A_P^-(k_x',k_y')\right|^2 \frac{c^2}{vk_x'} k_y' i\sqrt{k_x'^2+k_y'^2}\mu_0^{-1}(-k_y')[1-R_{PP}(\omega'=+vk_x')\exp(-2d\sqrt{k_x'^2+k_y'^2})] \\ &\quad\times[1+R_{PP}(\omega'=-vk_x')\exp(-2d\sqrt{k_x'^2+k_y'^2})] . \end{aligned} \tag{A2}$$

Collecting together the various pieces,

$$\begin{aligned}\int \mathbf{N}_z dx\,dy &= \int (E_xH_y-E_yH_x)dx\,dy \\ &= \sum_{k_x',k_y'} \left|A_P^-(k_x',k_y')\right|^2 \frac{c^2L_x'L_y'}{vk_x'} [k_x'^2+k_y'^2] i\sqrt{k_x'^2+k_y'^2}\mu_0^{-1} \\ &\quad\times[1-R_{PP}(\omega'=+vk_x')\exp(-2d\sqrt{k_x'^2+k_y'^2})][1+R_{PP}(\omega'=-vk_x')\exp(-2d\sqrt{k_x'^2+k_y'^2})] . \end{aligned} \tag{A3}$$

Finally recognizing various complex conjugates and seeing that the real arguments are antisymmetric in k_x, we see that there is no energy flux unless R is complex,

$$\begin{aligned}\int \mathbf{N}_z dx\,dy &= \int (E_xH_y-E_yH_x)dx\,dy \\ &= \sum_{k_x',k_y'} \left|A_P^-(k_x',k_y')\right|^2 \frac{c^2L_x'L_y'}{vk_x'} [k_x'^2+k_y'^2] i\sqrt{k_x'^2+k_y'^2}\mu_0^{-1} \\ &\quad\times\exp(-2d\sqrt{k_x'^2+k_y'^2})[-R_{PP}(\omega'=vk_x')+R_{PP}^*(\omega'=vk_x')] . \end{aligned} \tag{A4}$$

Substituting for A,

$$\begin{aligned}\int \mathbf{N}_z dx\,dy &= \int (E_xH_y-E_yH_x)dx\,dy \\ &= \sum_{k_x',k_y'} \frac{vq^2k_x'}{2c^2\varepsilon_0L_x'L_y'(k_x'^2+k_y'^2)} \frac{1}{2\varepsilon_0\mu_0} i\sqrt{k_x'^2+k_y'^2} \\ &\quad\times\exp(-2d\sqrt{k_x'^2+k_y'^2})[-R_{PP}(\omega'=vk_x')+R_{PP}^*(\omega'=vk_x')] . \end{aligned} \tag{A5}$$

Substituting for the reflection coefficient,

$$\begin{aligned}\int \mathbf{N}_z dx\,dy &= \int (\mathbf{E}\times\mathbf{H})_z dx\,dy = \int (E_xH_y-E_yH_x)dx\,dy \\ &= \int\int \frac{vq^2k_x'}{8\pi^2\varepsilon_0\sqrt{k_x'^2+k_y'^2}} \exp(-2d\sqrt{k_x'^2+k_y'^2})\mathrm{Im}\left[\frac{1-\varepsilon_2(\omega'=vk_x')}{1+\varepsilon_2(\omega'=vk_x')}\right] dk_x'dk_y' . \end{aligned} \tag{A6}$$

APPENDIX B

Here are the components of the fields for the case of a charged particle between two surfaces:

$$E_x(z=0-)=\sum_{k_x',k_y'} A_P^-(k_x',k_y')\frac{c^2}{\omega'}k_x'k_z' \frac{1-R_{PP}\exp(-2d\sqrt{k_x'^2+k_y'^2})}{1+R_{PP}\exp(-2d\sqrt{k_x'^2+k_y'^2})} \exp(ik_x'x+ik_y'y-i\omega' t) ,$$

$$E_y(z=0-)=\sum_{k_x',k_y'} A_P^-(k_x',k_y')\frac{c^2}{\omega'}k_y'k_z' \frac{1-R_{PP}\exp(-2d\sqrt{k_x'^2+k_y'^2})}{1+R_{PP}\exp(-2d\sqrt{k_x'^2+k_y'^2})} \exp(ik_x'x+ik_y'y-i\omega' t) , \tag{B1}$$

$$B_x(z=0-)=\sum_{k_x',k_y'} A_P^-(k_x',k_y')k_y'\exp(ik_x'x+ik_y'y-i\omega' t)\ ,$$

$$B_y(z=0-)=\sum_{k_x',k_y'} A_P^-(k_x',k_y')(-k_x')\exp(ik_x'x+ik_y'y-i\omega' t)\ . \tag{B2}$$

As in Appendix A we calculate the Poynting vector in region B, which represents half the total loss,

$$\int \mathbf{N}_z dx\,dy=\int (E_xH_y-E_yH_x)dx\,dy$$

$$=\sum_{k_x',k_y'}\left|A_P^-(k_x',k_y')\right|^2 L_x'L_y'\left\{\frac{c^2}{vk_x'}k_x'i\sqrt{k_x'^2+k_y'^2}\mu_0^{-1}(+k_x')-\frac{c^2}{vk_x'}k_y'i\sqrt{k_x'^2+k_y'^2}\mu_0^{-1}(-k_y')\right\}$$

$$\times\frac{1-R_{PP}(\omega'=vk_x')\exp(-2d\sqrt{k_x'^2+k_y'^2})}{1+R_{PP}(\omega'=vk_x')\exp(-2d\sqrt{k_x'^2+k_y'^2})}\ . \tag{B3}$$

Recognizing that we are summing over $\pm k_x'$ and that changing the sign of k_x' has the effect of taking the complex conjugate of ε,

$$\int \mathbf{N}_z dx\,dy=\int (E_xH_y-E_yH_x)dx\,dy$$

$$=\int\int \frac{vq^2k_x'}{8\pi^2c^2\varepsilon_0^2\mu_0\sqrt{k_x'^2+k_y'^2}}\mathrm{Im}\frac{1-R_{PP}(\omega'=vk_x')\exp(-2d\sqrt{k_x'^2+k_y'^2})}{1+R_{PP}(\omega'=vk_x')\exp(-2d\sqrt{k_x'^2+k_y'^2})}dk_x'dk_y'\ . \tag{B4}$$

Substituting the dielectric constant gives for the total loss to both surfaces,

$$2\int \mathbf{N}_z dx\,dy=26\int (E_xH_y-E_yH_x)dx\,dy$$

$$=2\int\int \frac{vq^2k_x'}{8\pi^2c^2\varepsilon_0^2\mu_0\sqrt{k_x'^2+k_y'^2}}\mathrm{Im}\frac{(1+\varepsilon_2)+(1-\varepsilon_2)\exp(-2d\sqrt{k_x'^2+k_y'^2})}{(1+\varepsilon_2)-(1-\varepsilon_2)\exp(-2d\sqrt{k_x'^2+k_y'^2})}dk_x'dk_y' \tag{B5}$$

or, in the limit of zero separation between the surfaces,

$$2\int \mathbf{N}_z dx\,dy=2\int (E_xH_y-E_yH_x)dx\,dy=\int\int \frac{vq^2k_x'}{4\pi^2\varepsilon_0\sqrt{k_x'^2+k_y'^2}}\mathrm{Im}\frac{1}{\varepsilon_2(\omega'=vk_x')}dk_x'dk_y'\ . \tag{B6}$$

[1] R. H. Ritchie and A. Howie, Philos. Mag. A **58**, 753 (1988).
[2] P. M. Echenique and J. B. Pendry, J. Phys. C **8**, 2936 (1975).
[3] T. L. Ferrell and P. M. Echenique, Phys. Rev. Lett. **55**, 1526 (1985).
[4] P. M. Echenique, A. Howie, and D. J. Wheatley, Philos. Mag. B **56**, 335 (1987).
[5] P. M. Echenique, J. Bausells, and A. Rivacoba, Phys. Rev. B **35**, 1521 (1987).
[6] C. A. Walsh, Philos. Mag. **59**, 227 (1989).
[7] J. C. Maxwell Garnett, Philos. Trans. R. Soc. London **203**, 385 (1904).
[8] S. J. Smith and E. M. Purcell, Phys. Rev. **92**, 1069 (1953).
[9] W. Lamb, D. M. Wood, and N. Ashcroft, Phys. Rev. B **21**, 2248 (1980).
[10] J. B. Pendry and A. MacKinnon, Phys. Rev. Lett. **69**, 2772 (1992).
[11] J. B. Pendry, J. Mod. Opt. **41**, 209 (1994).
[12] A. Otto, Phys. Status Solidi **22**, 401 (1967).
[13] R. Milne and P. M. Echenique, Solid State Commun. **55**, 909 (1985).
[14] R. Garcia Molina, A. Gras Marti, A. Howie, and R. H. Ritchie, J. Phys. C **18**, 5335 (1985).
[15] L. D. Landau and E. M. Lifshitz, *Electrodynamics of Continuous Media* (Pergamon, New York, 1960).
[16] A. Howie and C. A. Walsh, Microsc. Microanal. Microstruc. **2**, 171 (1991).
[17] M. Schmeits and L. Dambly, Phys. Rev. B **44**, 12 706 (1991).
[18] A. Rivacoba, N. Zabala, and P. M. Echenique, Phys. Rev. Lett. **69**, 3362 (1992).
[19] N. Zabala and P. M. Echenique, Surf. Sci. **209**, 465 (1989).
[20] Bob Greenler (private communication).